Losiak, A., et al., 2022, Small impact cratering processes produce distinctive charcoal assemblages: Geology, v. 50, https://doi.org/10.1130/G50056.1

Supplemental Material

Small impact cratering processes produce distinctive charcoal assemblages

A. Losiak[1,2],*, C. M. Belcher[2], J. Plado[3], A. Jõeleht[3], C. D. K. Herd[4], R. S. Kofman[4], M. Szokaluk[5], W. Szczuciński[5], A. Muszyński[5], E. M. Wild[6], S. J. Baker[1]

1Institute of Geological Sciences, Polish Academy of Sciences, Podwale 75, 50-449 Wroclaw, Poland
2wildFIRE Lab, Hatherly Laboratories, University of Exeter, Prince of Wales Road, EX4 4PS Exeter, UK;
3Department of Ecology and Earth Sciences, University of Tartu, Ravila 14A, 50411 Tartu, Estonia;
4Department of Earth and Atmospheric Sciences, University of Alberta, T6G 2E3 Edmonton, Canada;
5Geohazards Lab, Institute of Geology, Adam Mickiewicz University, Bogumiła Krygowskiego 12, 61-680 Poznań, Poland
6VERA Laboratory, Faculty of Physics—Isotope Research, University of Vienna, Waehringer Strasse 17, 1090 Vienna, Austria.

Supplementary Materials and Methods

Dating of Impact Craters:

In the Kaali Main Crater, the ^{14}C age of the deepest organic material within the crater, as well as all impact charcoals are of the same ^{14}C age of 3.5 ka (Losiak et al. 2016). Additionally, impact charcoals from a different crater of the same strewn field: Kaali 2/8, that is located 600 meters, have the same age (Losiak et al. 2018). Impact charcoals from Morasko Main are roughly of the same age of ~5 ka (Szczucinski et al. 2016) as palynological (Tobolski 1976) and ^{14}C (Stankowski 2010) dating of sediments within the crater. The Whitecourt crater was dated only using charcoals from the ejecta (Herd et al. 2008), so it is not possible to determine if their ages overlap with the independently determined age of the crater. However, both dated samples from other sides of the crater yield overlapping ages of 1130 ± 25 and 1080 ± 25 14C yr B.P., which suggest that they were formed at the same time.

Detailed descriptions of the charcoal samples:

Impact charcoal samples - Charcoal samples were collected together with the surrounding sediment by A.L. on a series of field campaigns between 2014 and 2018 (and later separated and processed in the lab) with the exception of the samples from Whitecourt that were collected by C.H. and R.K, and the Morasko samples were partially provided by A.M., W.S. and M.S and collected by A.L.

All charcoal samples associated with ejecta (called later "impact charcoals") were taken in the same geomorphological setting in respect to the crater - from the ejecta layer between the crater rim and up to ~0.5 x diameter outwards. Vertically the charcoals were present mainly in the lowest part of the ejecta layer (Fig. 1, see Losiak et al. 2016, Losiak et al. 2018, Szokaluk et al. 2019, Kofman et al. 2010 for detailed descriptions of ejecta sequences and charcoal distribution in the ejecta). Impact charcoals are couple of mm in diameter (Fig. 1 Kaali_17_47 from Kaali Main, M.m.2016_2b from Morasko), although some larger particles were also found (Fig. S1. Kaali8/2_1_47 from Kaali 2/8 where they were particularly common, M.m.2016_1 from Morasko). Within the Kaali strewn field, where unconsolidated glacial till overlays consolidated Silurian dolostones, some charcoals were found directly on the fresh-looking crushed dolomite clasts (most probably fragmented during the impact event). The average share of charcoal in the "charcoal-rich" section of the ejecta blanket is very low; usually ~0.05 wt % within the particularly enriched zone. In other places within ejecta charcoals are present as highly dispersed single particles or groups of particles. Locally, a higher densities of charcoal grains are possible; they seem to correspond to a fragments of a single branch that were not fragmented and intermixed during the ejecta formation, but were crushed into smaller pieces after charring within sediment (Fig. S1).

Fig. S1. Zones that are particularly charcoal-rich zones within proximal ejecta of Kaali 2/8 crater (Estonia). When these larger pieces were removed from the sediment, they disintegrate into small pieces (as visible on photo B). Based on particle morphology they seem to be formed from a single piece of branch that was buried within ejecta, that were later charred and crushed by the overlaying sediment.

Outside the charcoal-rich zone (defined both by the horizontal distance from the crater and by vertical position within ejecta blanket) on similar depths below the surface (>50 cm) there is no noticeable charcoal, although locally some particles from the soil appear to have been bioturbated downwards and occur close to root pseudomorphs.

Charcoal reflectance measurement:

Reflectance (Ro) of charcoal can be used to determine the level of graphitization of charcoal (Ascough et al. 2010) which relates to the total amount of thermal energy delivered to the sample (Belcher et al. 2018). The more energy used to create a given fragment of charcoal, the higher is its reflectivity and the brighter it appears in the reflectance microscope (Fig. 2, Fig. S3). The sampled charcoals were embedded in cold-mounting polyester resin, then ground and polished using a Buehler MetaServ 250 grinder–polisher (Buehler, Neckar, Germany). First, the top surface of the resin was ground down using a silicon carbide disc (50-µm grain size) until the surface of the charcoal was exposed. This surface was then re-impregnated with resin and placed in a vacuum to ensure that resin was pulled into the cells of the char. Once resin cured, the top surface was ground down again, and then polished using a Kemet synthetic silk polishing pad with Kemet 3-µm diamond suspension (Kemet International, Maidstone, UK), to remove any scratches. All charcoal particles were orientated similarly in the resin so that the same parts of the surface of the wood was analyzed. Typically, such that the microscope was able to view the length of the trachieds in the wood (e.g. see Fig. S3). Each particle therefore shows a cross-section from the edge surfaces of the particle e.g. Fig. S3 top left image, and moves away from the edge of the particle. The polished charcoals were analyzed using a Zeiss Axio-Scope A1 optical microscope, with a TIDAS-MSP 200 microspectrometer, at the wildFIRE Lab at the University of Exeter, under oil (RI 1.514) and calibrated using three synthetic standards Strontium Titanite (5.41% Ro), Gadolinium Gallium Garnet (GGG) (1.719% Ro) and spinel (0.42% Ro). Samples were studied using a x50 objective (with x32 eyepiece magnification), and reflectance measurements were obtained manually using MSP200 v 3.47 software. 30-50 manual reflectance measurements were taken along transects crossing the entire particle (i.e. edge to edge), at locations where cell wall junctions were thick enough for the measurement

(>5 μm radius) and charcoal was polished well enough. Because of that, spacing between measuring points depends on the: 1) type of wood, 2) slight variations in orientation of the particle, 3) quality of polishing at given site (what also depends on the type of wood). Each sample consisted of at least three individual pieces (usually five), and each piece was measured in at least 35 points (usually 50). Representative color micrographs were taken using an AxioCam 105 color 5-megapixel eyepiece camera attached to the reflectance microscope using Zeiss Zen software (Fig. 2).

Supplemental Figures and Tables

Table S1. A list of impact indicators used to prove extraterrestrial origin of small Quaternary impact craters <200m in diameter on Earth. The list does not include locations where only terminal pits exist (those are formed when the bolide is slowed down below the speed of sound in the target material usually <1-2 km/s) such as Sterlitamak. Douglass is also not included since it is significantly older (280 Ma) than other features (Kenkmann et al. 2018).

Crater Parameters					Impact Indicators									References
Crater	Max diameter [m]	Age[a]	Impactor type	No craters	Meteorite	Geochemical traces	Shater cones	Planar Deformation Features	Coesite	Melt/ diapletic glass	Overturned sequence	Witnessed	*Charcoal in proximal ejecta*	
Carancas	14	*2007	H4-5	1	M							W		Kenkmann et al. 2009
Haviland	15	0.2 ka	Pallasit	1	M									Shoemaker et al. 1990
Dalgaranga	24	?	M.siderite	1	M								*?Ch*	Hamacher et al. 2013
Sikhote Alin	27	*1947	IIAB	5 +n	M							*W***		Krinov 1971
Whitecourt	36	1,1 ka	IIIAB	1	M			PF?			Ov		***Ch***	Herd et al. 2008
Kamil	45	? / <4ka	Iron,	1	M			PDF	C	Mt				Folco et al. 2018
Sobolev *	53	? / <1	?	1		?Ni	?Sh			?Mt	Ov		*?Ch*	Khryanina 1981
Campo d. Cielo	65x105	4 ka	IAB	4 +n	M						Ov		*?Ch*	Cassidy et al. 1964
Ilumetsä *	80	7 ka	?	2		?Ni							***Ch***	Losiak et al. 2020.
Veevers	80	?	IIAB	1	M									Shoemaker et al. 2005
Morasko	100	5 ka	IAB-MG	7	M						Ov		***Ch***	Szokaluk et al. 2019
Kaali	110	3,5 ka	IAB	8	M		Sh				Ov		***Ch***	Losiak et al. 2016
Wabar	116	? / *XIX	IIIA	5	M			PDF?	C	Mt				Gnos et al. 2013
Henbury	157	4,2 ka	IIIAB	13	M					Mt	Ov			Shoemaker et al. 2005
Odessa	168	63 ka	IAB	5	M					Mt				Holliday et al. 2005
Boxhole	170	3 ka	IIAB	1	M									Shoemaker et al. 2005

[a] from Schmieder and Kring 2020

* suspected structures

** the atmospheric entry was witnessed, not the impact itself

Table S2. Comparison of reflectance properties of the populations of wildfire and impact charcoals from different locations. No single charcoal particle can be identified as formed by heating in a proximal ejecta blanket, but wildfire and impact charcoal populations clearly differ from each other.

Location	median	st. dev.	particles	measurements	% of points st.dev > 0.15 particles		% of particles with median Ro >1.15% particles		% of particles with 95th percentile Ro >1.4% particles		% of particles with 75th percentile Ro >1.2% particles	
	all measurements				#	%	#	%	#	%	#	%
Craters confirmed	0,76	0,22	347	12988	7	2,0	1	0,3	0	0,0	2	0,6
Kaali Main	0,78	0,2	117	5240	2	1,7	1	0,9	0	0,0	1	0,9
Kaali 2/8	0,74	0,15	131	3538	2	1,5	0	0,0	0	0,0	0	0,0
Morasko	0,86	0,18	50	1914	1	2,0	0	0,0	0	0,0	1	2,0
Whitecourt	0,5	0,23	49	2296	2	4,1	0	0,0	0	0,0	0	0,0
Wildfires	0,82	0,44	513	23495	164	31,5	117	22,5	131	25,2	151	29,0
Pine Point, USA	1,24	0,26	14	449	2	14,3	6	42,9	5	35,7	9	64,3
Triangle, USA	1,58	0,42	29	869	15	51,7	26	89,7	25	86,2	27	93,1
near Ilumetsa L.	1,01	0,41	75	2263	16	21,3	23	30,7	20	26,7	26	34,7
near Ilumetsa S.	0,83	0,51	81	3443	15	18,5	15	18,5	16	19,8	17	21,0
central Sweden	0,76	0,45	19	2566	10	52,6	4	21,1	5	26,3	6	31,6
Ferndown, UK	0,94	0,45	45	2422	27	60,0	12	26,7	18	40,0	20	44,4
Wareham, UK	0,84	0,31	211	9981	50	23,7	20	9,5	25	11,8	29	13,7
Moon Pass, USA	0,99	0,53	39	1502	29	74,4	10	25,6	16	41,0	16	41,0

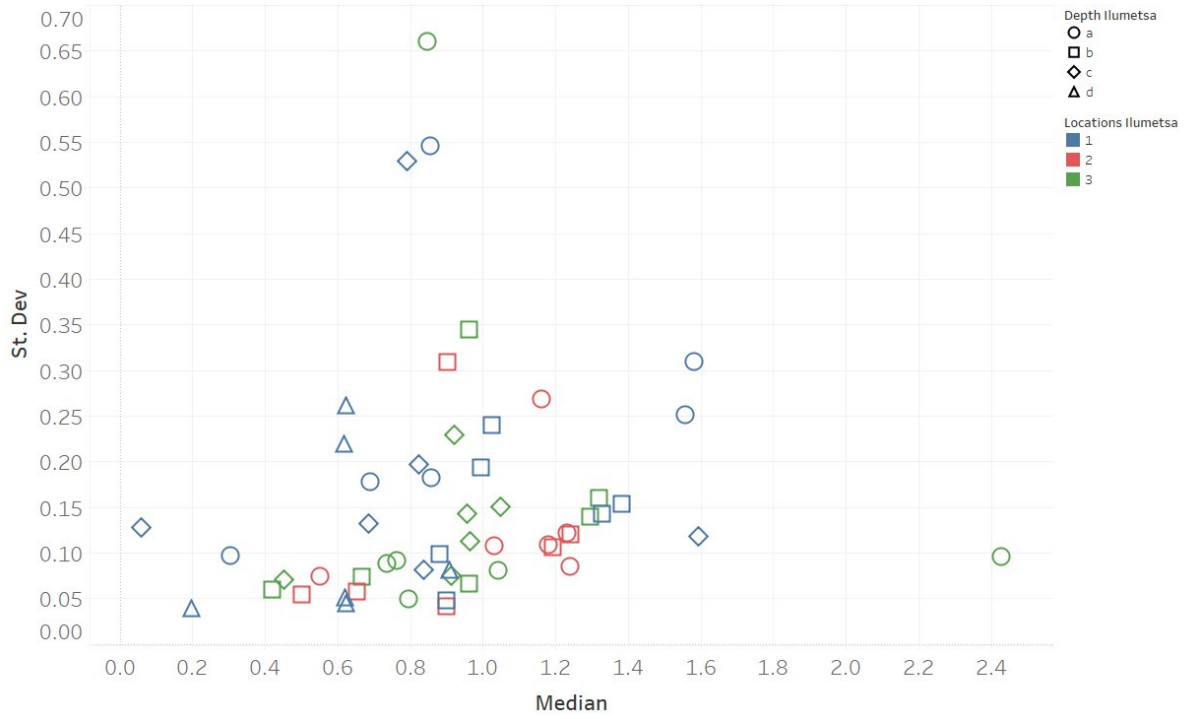

Fig. S2. Expansion of the data for the Ilumetsa soil samples from Figure 2 showing the variation in charcoal reflectance of soil charcoals from 3 sample 'pits' over 4 different depths per soil section for Illumetsa in Estonia. Charcoals were collected on the soils that had developed on the proximal ejecta blanket of Ilumetsa Large proposed impact crater (Losiak et al. 2020). Data from both Ilumetsa Large and Small are presented on Fig 2. The location of each sample 'pit' is indicated by a different color (blue, red, green) and the different depths are denoted by different symbols: circle = 0-10cm, square = 10-20cm, diamond = 20-30cm and triangle = 30-40 cm.

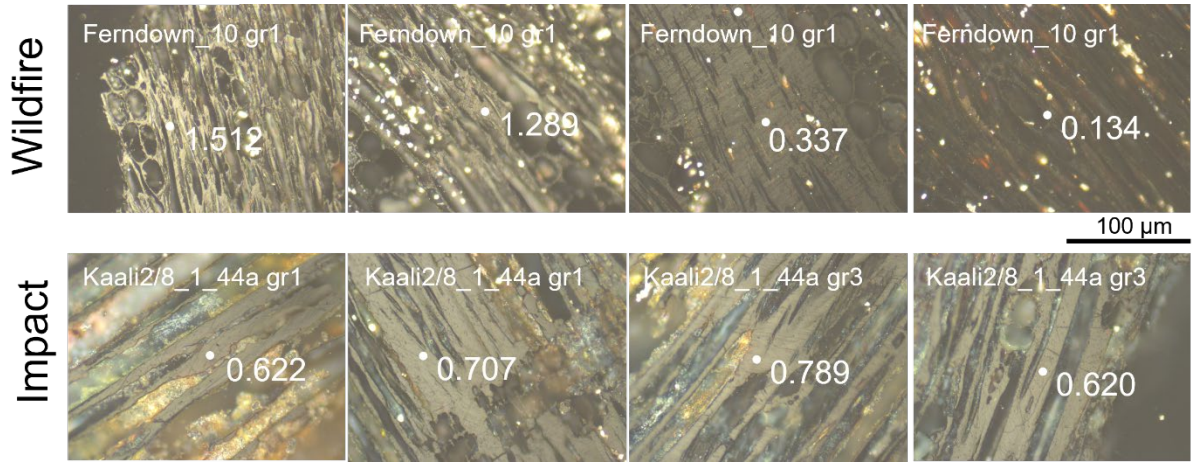

Fig. S3. Comparison of wildfire and impact charcoals as seen in reflectance light (all microscope, microspectrometer and camera settings remained the same). Measurements are taken on thick sections of well-polished cell walls. All images in the upper section of the figure 3S show different places within of a single, 3 mm in length, charcoal piece from a 2018 wildfire at Ferndown Common, UK. It can be seen that this particle experienced a high heat flux to it's surface (top far left image with Ro = 1.512%) but moving into the centre of the particle (top far right image) the reflectance and therefore the level of charring decreases (Ro = 0.134%). The reddish color visible at the top-right image is characteristic to wood that was not fully transformed to charcoal. This wide range of measured reflectance values within a single particle is typical of the wildfire particles (from 1.512% left-outer to 0.134% right-inner). The bottom line of images shows examples of impact charcoals taken from two particles from a single sample Kaali 2/8_1_44a; they show a typical range of reflectance measurement from 0.620% up to 0.789% where reflectance is similar (relatively homogeneous) throughout each particle and similar between the two particles.

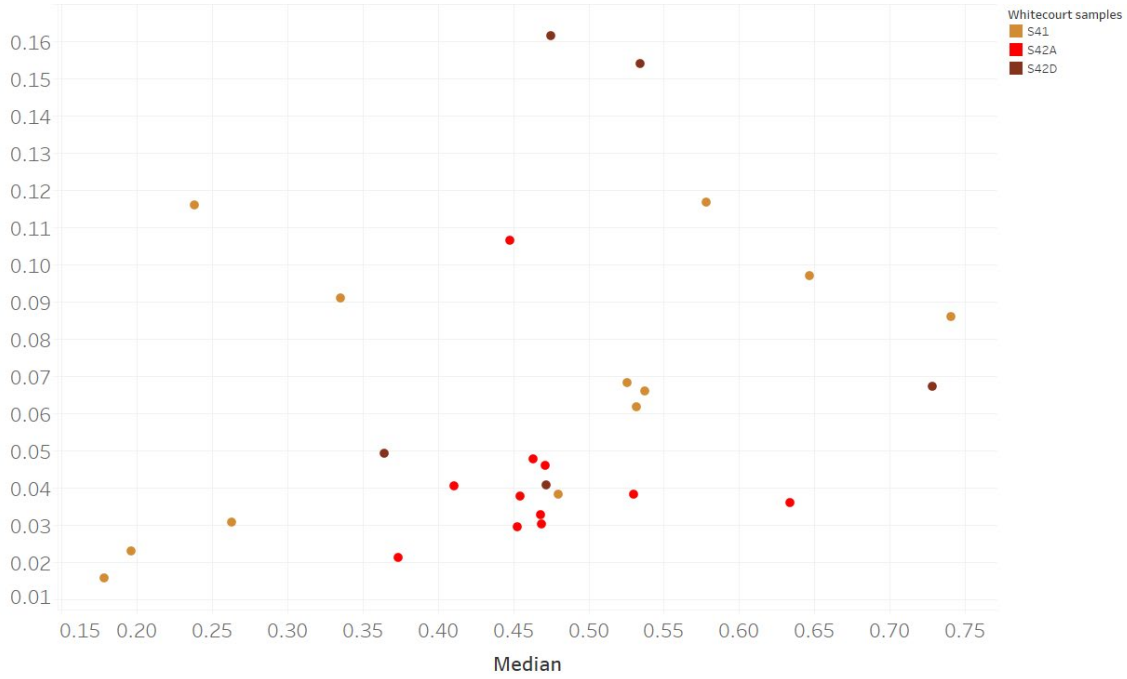

Figure S4 – variations in median charcoal reflectance with distance from the crater rim at Whitecourt, Canada. Y – axis is Standard Deviation. Light brown dots (S41) are sampled by the crater rim, red 7m from the rim (S42A) and dark red 14m from the crater rim (S42D).

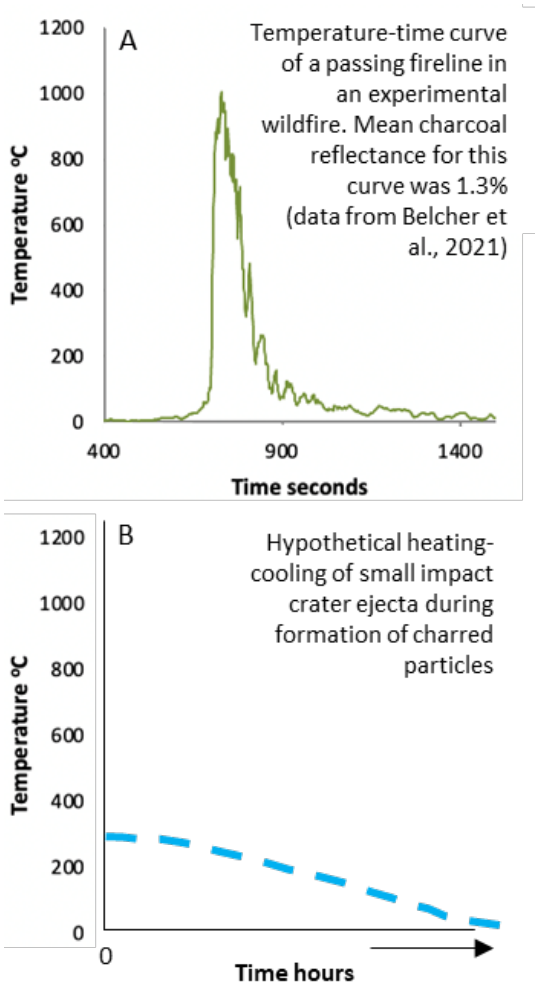

Figure S5. A) Temperature-time curve for a thermocouple attached to a pitch pine tree during an experimental wildfire showing the nature of the energy regime causing charring in wildfires (data from Belcher et al., 2021). B) Hypothetical (for illustrative purposes only) heating and cooling of small impact crater ejecta that could lead to the charring of entrained organic material. Note low maximal temperature, and hours long time of exposure to elevated temperature.

Additional references cited in the Supplementary Material

1. Hamacher, D. W., O'Neill, C., 2013, The discovery and history of the Dalgaranga meteorite crater, Western Australia. Australian J. Earth Sci. 60, 637-646.
2. Holliday, V. T. , et al., 2005, Age and effects of the Odessa meteorite impact, western Texas, USA. Geology 33, 945-948.
3. Kenkmann, T., Sundell, K.A., Cook, D., 2018, Evidence for a large Paleozoic Impact Crater Strewn Field in the Rocky Mountains. Sci. Rep. 8: 13246.
4. Liiva, A., Kessel, H., and Aaloe, A. Age of the Ilumetsa craters. Eesti Loodus, 12, 762-764. In Estonian. (1979).Shoemaker, E. M., MacDonald, F. A., Shoemaker C. S., 2005, Geology of five small Australian impact craters. Austral. J. Earth Sci. 52, 529 – 544.
5. Stankowski, W. Meteoryt Morasko, osobliwość obszaru Poznania/ Morasko Meteorite, a curiosity of the Poznań region. Wyd. Nauk.UAM, Ser. Geologia 19, Poznań (2010).
6. Szczuciński, W. et al., 2016, Identification and dating of small impact crater ejecta deposits, case of Morasko craters, Poland (abstract). 32nd IAS International Meeting of Sedimentology, 23–25 May 2016, Marrakesh, Morocco.
7. Tobolski, K. Palynological investigations of bottom sediments in closed depressions. in Meteorite Morasko and the region of its fall (eds. Hurnik H.) 21–26 (Wydawnictwo Naukowe Uniwersytetu im. Adama Mickiewicza, 1976).